Available online at www.sciencedirect.com

ScienceDirect

Procedia Materials Science 8 (2015) 510 – 518

Procedia Materials Science

www.elsevier.com/locate/procedia

International Congress of Science and Technology of Metallurgy and Materials, SAM - CONAMET 2013

Anodic Behavior of Alloy 22 in Bicarbonate Media: Effect of Alloying

Zadorozne Natalia S.[a-c], Giordano Mabel C.[b,c], Rebak Raúl B.[d], Ares Alicia.E.[a], Carranza Ricardo.M.[b,c]

[a]Instituto de Materiales de Misiones - IMAM (CONICET - UNaM)
[b]Gerencia Materiales Centro Atómico Constituyentes, Av. General Paz 1499, (B1650KNA) San Martín, Buenos Aires, Argentina.
[c]Instituto Sabato – Universidad Nacional del Gral San Martín.
[d]GE Global Research, 1 Research Circle, CEB2505, Schenectady, NY 12309, USA.

Abstract

The alloy 22 (UNS N06022) is one of the candidates for the manufacture of containers of radioactive waste high level. These containers provide services in natural environments characterized by multi-ionic solutions, it is estimated they could suffer three types of deterioration: general corrosion, localized corrosion (specifically crevice) and stress corrosion cracking (SCC). It has been confirmed to produce cracking, requires the presence of bicarbonate and chloride ions. It has also determined that susceptibility to SCC could be related to the occurrence of an anodic peak in the polarization curves in these media to at potentials previous transpassive zone.

The aim of this work is to study the anodic behavior of alloy 22 and its alloying effect in different media containing bicarbonate and chloride ions in different concentrations and temperatures.

Polarization curves were made of alloy 22 (Ni-22% Cr-13% Mo), Ni-Mo (Ni-28, 5% Mo) and Ni-Cr (Ni-20% Cr) under the following conditions: 1 mol/L NaCl at 90 °C, and 1.148 mol/L $NaHCO_3$, 1.148 mol/L $NaHCO_3$ + 1 mol/L NaCl, 1.148 mol/L $NaHCO_3$ + 0.1 mol/L NaCl at 90 °C, 75 °C, 60 °C and 25 °C.

It was found that the alloy 22 has a current peak in the anodic at potential previous to transpassive zone, only when the medium has bicarbonate ions. Curves performed in 1 mol/L NaCl did not show any anodic peak, in any of the alloys tested. The curves made to alloys Ni-Mo and Ni-Cr in the media with bicarbonate ions, allowed to determine that Cr, is responsible for the appearance of the anodic peak in the Alloy 22. The curves of alloy B-3 showed no current peak in the conditions studied. The potential, at which the peak appears in the Alloy 22 and Ni-Cr alloy, increases with decreasing temperature. It also presents a variation of the peak with the composition of the solution. When the chloride ion is added to bicarbonate solution, the peak is shifted potential and higher current densities, depending on the concentration of added chloride ions.

Selection and peer-review under responsibility of the scientific committee of SAM - CONAMET 2013

Keywords: nickel based alloy; UNS N06022; bicarbonate; anodic behavior; alloying.

Selection and peer-review under responsibility of the scientific committee of SAM - CONAMET 2013
doi:10.1016/j.mspro.2015.04.103

1. Introduction

Ni-Cr-Mo alloys constitute one of the various families originated when nickel is alloyed with different metals. Within this family we found the alloy 22 (56.58% Ni-22, 26% Cr-13, 9% Mo-3, 1% W-3, 81% Fe), which has been designed to resist corrosion in both oxidative and reductive conditions, in the most commonly environment in industry. Through of these properties to resist corrosion is one of the candidates for the manufacture of containers of high-level nuclear waste. (Rebak 2003, Gordon 2002).

Geological repositories are based on the multi-barrier principle, which consists to interpose a series of barriers, natural and engineering between the wastes and the biosphere (Witherpoon 2006, Bodvarsson 2003). Natural barriers have to contribute to isolation of the waste by minimizing the amount of water entering the tank and limiting the transport of the waste through the natural system, for which it should be located above and below the stable geological formations. Engineering barriers are designed specifically to prolong the isolation of wastes and limit their release potencial (Bodvarsson 2003). The main engineering barrier is the container. Since containers will provide services to natural environments characterized by multi-ionic aqueous solutions (Witherpoon 2006, Gordon 2002), it is estimated that this material could suffer three different types of deterioration: general corrosion, localized corrosion (specifically crevice) and stress corrosion cracking (SCC).

Generalized and localized corrosion (crevice corrosion) has been extensively studied in the presence of solutions which simulate groundwater components (Rebak 2005, Dunn 2004, Dunn 2003, Cragnolino 2003, Rodrigruez 2009, Rodriguez 2010).

On the contrary, have been conducted relatively few experimental studies to understand the processes of stress corrosion of the alloy 22. Researchers from Lawrence Livermore National Laboratory studied the potential range of susceptibility to SCC of alloy 22 in simulated groundwater using several constant deformation and tensile tests at low speeds. They varied potentials, chemistry of solution and temperature (Estill 2003, Fix 2003, Fix 2004, King 2004). Their results suggest that alloy 22 is susceptible to SCC at a range of potentials between 0.3 and 0.4 VSSC ($V_{SSC} = V_{ENH} + 0{,}198V$) in concentrated groundwater and above 65 ° C. They did not observe SCC in basic saturated groundwater neither can in the acidified.

Most recently Chiang et al. (2005, 2006) studied the effect of certain components of groundwater on SCC concentrated on alloy 22 at 95 °C. Testing suggest that is essential the coexistence of bicarbonate and chloride ions to produce SCC. The susceptibility appears to increase with increasing chloride concentration. In these studies it was found that the probability of cracking is low at corrosion potential in all media tested.

The necessity of the presence of bicarbonate ions to produce cracking was confirmed by researchers at the South West Research Institute (Skukla 2006) who indicated that only at pH values between 7 and 11 the bicarbonate concentration is important. Experimentally it found that SCC occurred in a pH range between 8.5 and 10.5. They determined that SCC susceptibility may be related to the appearance in these media of anodic peak into polarization curves, at potential previous to transpassive zone. The intensity of the anodic peak increased with increasing bicarbonate concentration in solution. Dunn et al showed that when alloy 22 undergoes SCC in the presence of bicarbonate and chloride, is observed presence of a thicker anodic film on the surface of the alloy, and this film is chromium depleted with respect to the base alloy. They suggested causality between this experimental evidence (Dunn 2006, Chiang 2007). Previous studies concluded that the presence of this anodic peak in alloy 22 must be due to one of the major alloying (Zadorozne 2012).

Because SCC of this alloy could be related to the appearance of the anodic peak, the aim of this work is focused on studying the effect of alloying elements of alloy 22 on their behavior, in different media containing bicarbonate and chloride ions, in different concentrations and temperatures. This will relate the anodic peak current in the polarization curves of the alloy 22 with their major alloying elements, and further, determining the characteristics and dependencies of anodic peak with temperature and concentration of the medium. It is expected to characterize the conditions for the appearance of anodic Peak, then compared with tensile tests of alloy 22 in the same conditions and determine whether nickel or any of the alloying is responsible for the SCC of alloy 22.

2. Experimental Procedure

The chemical compositions of the tested alloys in weight percent are listed in Table 1. The samples used were in the form of parallelepipeds, a variation of the ASTM G 5 (AST; G5-94, 2004) sample, with approximate dimensions of 12 mm x 12 mm x 15 mm. Each sample was screwed to a metal rod that was used as electrical contact, which was introduced in a glass test tube holder and was isolated from the solution with a PTFE gasket. The exposed area to the solution was approximately 10 cm^2. The samples had a finish grinding of abrasive SiC paper number 600 and were degreased in acetone and washed in distilled water within the hour prior to testing. Figure 1 shows a schematic of samples.

Table 1. Chemical composition of Nickel-based alloys (Weight %)

Alloy	Ni	Cr	Mo	W	Fe	Si	Mn	C	S	Other
22	56.58	22.26	13.90	3.15	3.81	0.02	0.24	0.004	0.001	Co: 0.2
Ni-Cr	Bal.	20								
Ni-Mo	Bal.		28.5							

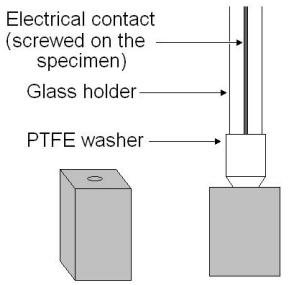

Fig. 1. Schematic of the prismatic samples.

All the electrochemical tests were conducted in a one-liter, three-electrode vessel. The nitrogen (N_2) was purged through the solution 1 hour prior to testing and was continued throughout the entire test. A water-cooled condenser combined with a water trap was used to avoid evaporation of the solution and to prevent the ingress of air (oxygen). The temperature of the solution was controlled by immersing the cell in a water bath, which was kept at a constant temperature. The reference electrode was a saturated calomel electrode (SCE) ($V_{SCE} = V_{SHE} + 0.242V$). The reference electrode was connected to the solution through a water-cooled Luggin probe. The counter electrode consisted in a flag of platinum foil (total area 50 cm^2) spot-welded to a platinum wire. All the potentials in this paper are reported in the SCE scale.

The solution used were: 1.148 mol/L $NaHCO_3$, 1.148 mol/L $NaHCO_3$ + 0.1 mol/L NaCl, 1.148 mol/L $NaHCO_3$ + 1 mol/L NaCl and 1 mol/L NaCl. The choice of these environments was based in multi-ionic solution called SCW (Simulated Concentrated Water), used in the works on SCC in alloy 22. The pH of the solutions was kept in a range between 8 and 8.5 at the start of the test. The test temperatures were 25ºC, 60ºC, 75ºC and 90ºC. The potentiodynamic polarization curves were performed using a scan rate of 0.167 mV/ s.

3. Results

In a first step of this work, polarization curves of 22, Ni-Cr and Ni-Mo alloys were performed, in an environment free of bicarbonate ions. This was done to corroborate studies due by Dunn et al. (2006), who affirm that when

bicarbonate ions are present in the medium the anodic peak only occurs. Figure 2 shows polarization curves of alloys 22, Ni-Cr and Ni-Mo in 1 mol/L NaCl at 90°C. Was not observed any anodic peak previous to transpassive zone in the materials tested. Is noteworthy that the best corrosion performance is the alloy 22 (Ni-Cr-Mo) compared to alloys which are constituted only with one of the major alloying elements (Ni-Cr and Ni-Mo). Was not observed any anodic peak previous to transpassive zone in the materials tested. Of note is the best corrosion behaviour of the 22 (Ni-Cr-Mo) alloys compared to that alloys which consist only of one of the major alloying elements (Ni-Cr and Ni-Mo). The alloy 22 showed a large area of passivity reaching transpassive zone at potentials over 200 mV_{SCE}. Ni-Cr alloy showed a short passivity zone compared to alloy 22, when reached potentials close to 0 mV_{SCE}, the current increased abruptly. Unlike the 22, Ni-Cr, Ni-Mo alloys at no time present a passive zone. After reaching its corrosion potential, current density increased continuously. Once finished the tests, the samples were cleaned to observe under the microscope. Alloy 22 showed no signs of pitting, while Ni-Cr and Ni-Mo alloys showed pitting on the entire surface to the naked eye.

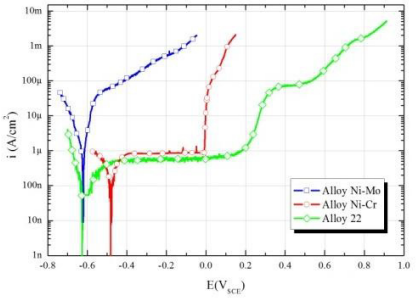

Fig. 2. Polarization curves of alloys 22, Ni-Mo and Ni-Cr performed in 1 mol / L $NaHCO_3$ at 90 °C.

Then the alloys were studied in media containing bicarbonate and chloride, at different concentrations and temperatures. In Figures 3 to 5 are shown the polarization curves of the alloy 22, held in 1.148 mol/L $NaHCO_3$, 1.148 mol/L $NaHCO_3$ + 0.1 mol/L NaCl and 1.148 mol/L $NaHCO_3$ + 1 mol/L NaCl respectively, at 25ºC, 60ºC, 75ºC and 90ºC. Similarly, Figures 6 to 8 show the polarization curves of the Ni-Cr alloy, carried out in 1.148 mol/L $NaHCO_3$, 1.148 mol/L $NaHCO_3$ + 0.1 mol/L NaCl y 1.148 mol/L $NaHCO_3$ + 1 mol/L NaCl, respectively, at 25ºC, 60ºC, 75ºC and 90ºC. Finally, in Figures 9 to 11 are shown the polarization curves of the Ni-Cr alloy, carried out in 1.148 mol/L $NaHCO_3$, 1.148 mol/L $NaHCO_3$ + 0.1 mol/L NaCl and 1.148 mol/L $NaHCO_3$ + 1 mol/L NaCl at the same temperatures.

It was observed that the alloy 22 presented an anodic peak prior to transpassive zone in all media and temperatures.

When the temperature was 90 °C, the current density, which was filed approximately constant in the passivity zone, sharply increased and then decreases forming the peak current. This decrease in current went deeper as the temperature was increased. At the lowest test temperature, the diminishing in current after the peak was only 50% of the decline which was exhibited at the highest temperature. This behavior was observed for all media tested. After the peak, was showed a zone where the current again remain constant. Below are presented the transpassivity of material. Furthermore it was observed that for all three media tested, the corrosion potential increased with decreasing temperature.

Ni-Cr alloy showed a very similar behavior to alloy 22. This alloy presented an anodic peak in all media and all temperatures. We observed the same features present in the alloy 22, both in the passivation as in the post-peak zone. However, an exception appeared when we tested in 1.148 mol/L $NaHCO_3$ + 1 mol/L NaCl at 25°C. In this case, once the current began to rise after the passive zone, not stopped and thus do not form any peak.

Ni-Mo alloy showed a completely different behavior. In any of the tested conditions presented an anodic peak. Ni-Mo alloy showed a significant peak of active/passive transition followed by a region where the current density decreases as the potential increases. When reaching potential higher than 500mVECS, the current density increases resulting in the transpassivity of material. This behavior is shown in the three media tested and temperatures of 60 °C, 75 °C and 90 °C. When the test temperature was 25 °C, the Ni-Mo alloys no showed peak of active/passive

transition. Rather, presented passivity zone where the current density was kept constant. After 300 mV_{SCE}, the current increased, creating a plateau in the curve. At potentials close to 900mVECS the alloy presented transpassivity. This behavior was observed in the three concentrations of media tested.

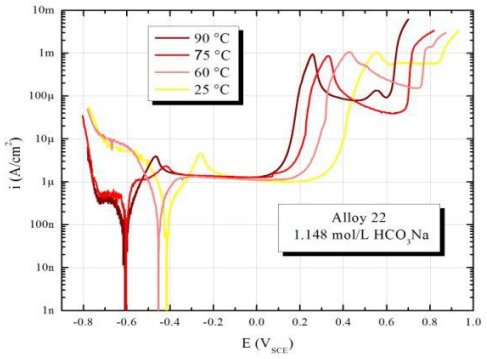

Fig. 3. Polarization curves of alloy 22 in 1,148 mol/L $NaHCO_3$ at 25ºC, 60ºC, 75ºC and 90ºC.

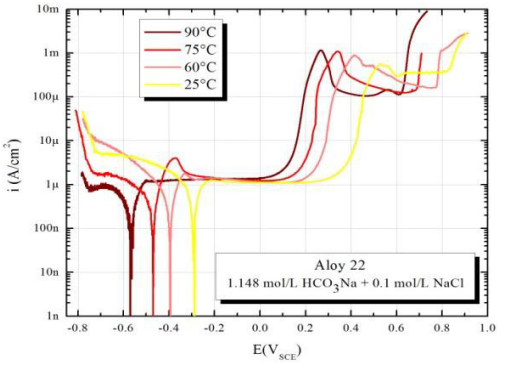

Fig. 4. Polarization curves of alloy 22 in 1,148 mol/L $NaHCO_3$ + 0.1 mol/L NaCl at 25ºC, 60ºC, 75ºC and 90ºC.

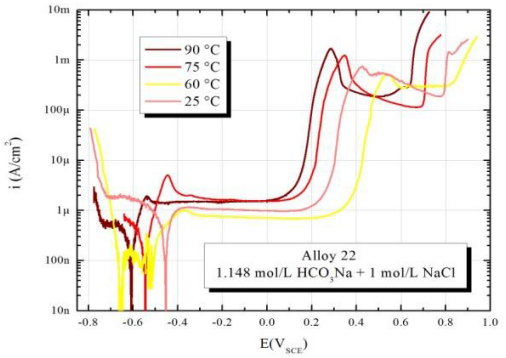

Fig. 5. Polarization curves of alloy 22 in 1,148 mol/L $NaHCO_3$ + 1 mol/L NaCl at 25ºC, 60ºC, 75ºC and 90ºC.

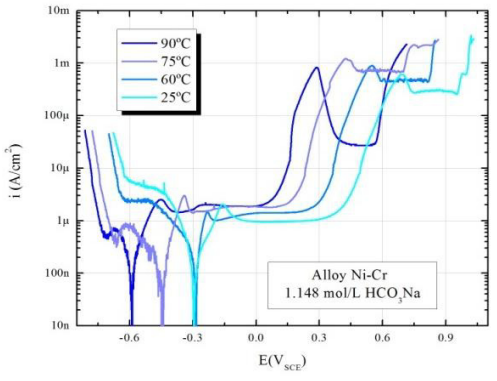

Fig. 6. Polarization curves of Ni-Cr alloy in 1.148 mol/L $NaHCO_3$ at 25ºC, 60ºC, 75ºC and 90ºC.

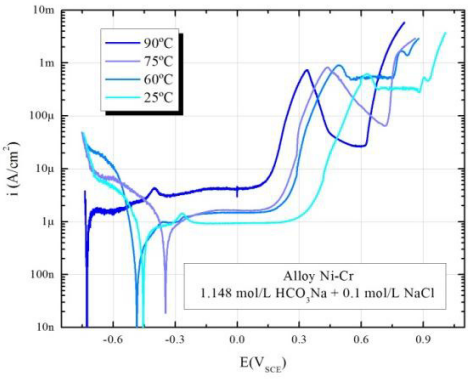

Fig. 7. Polarization curves of Ni-Cr alloy in 1.148 mol/L $NaHCO_3$ + 0.1 mol/L NaCl at 25ºC, 60ºC, 75ºC and 90ºC.

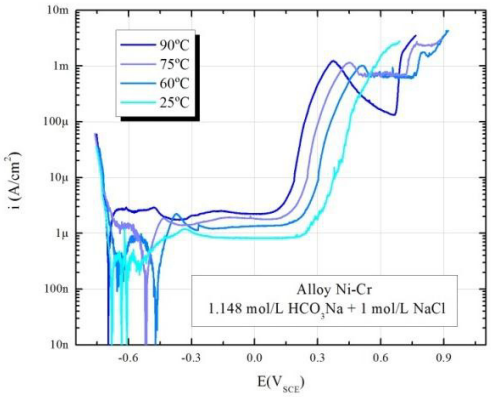

Fig. 8. Polarization curves of Ni-Cr alloy in 1.148 mol/L $NaHCO_3$ + 1 mol/L NaCl at 25ºC, 60ºC, 75ºC and 90ºC.

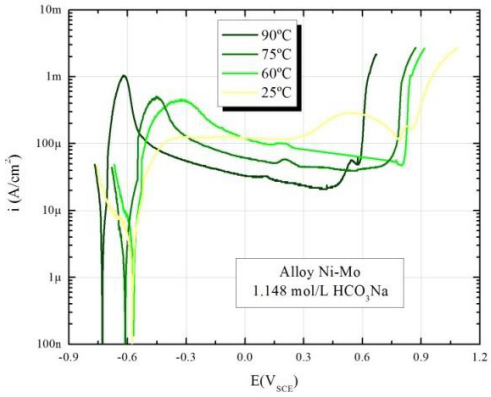

Fig. 9. Polarization curves of Ni-Mo alloy in 1.148 mol/L $NaHCO_3$ at 25ºC, 60ºC, 75ºC and 90ºC.

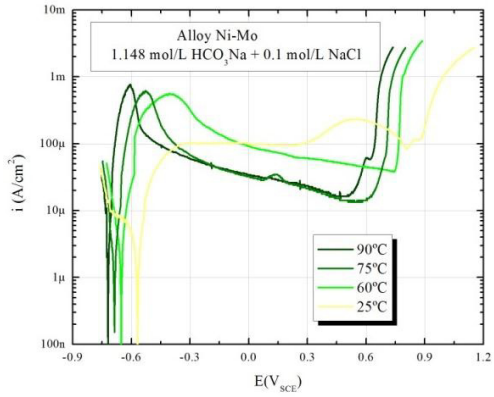

Fig. 10. Polarization curves of Ni-Mo alloy in 1.148 mol/L $NaHCO_3$ + 0.1 mol/L NaCl at 25ºC, 60ºC, 75ºC and 90ºC.

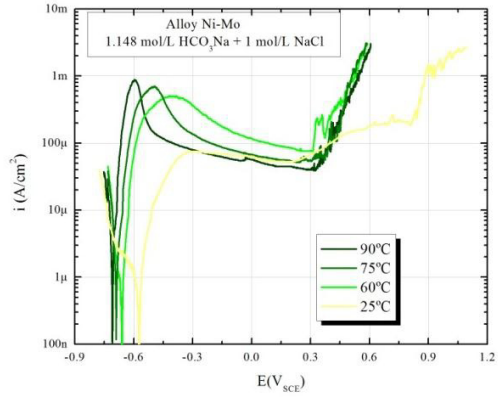

Fig. 11. Polarization curves of Ni-Mo alloy in 1.148 mol/L $NaHCO_3$ + 1 mol/L NaCl at 25ºC, 60ºC, 75ºC and 90ºC.

Once finished the tests, samples were cleaned using ultrasound and observed by optical microscope. The samples that showed most damage were those of Ni-Mo. In addition, there was a marked increase in surface damage of samples when the concentration of chloride increased in the medium tested.

From polarization curves values of potential and current density at which the anodic peak occurs, were obtained. The variation of potential and current density of peak was analyzed as a function of temperature, concentration of solution and composition of alloys.

4. Discussion

4.1. Effect of alloy composition on the appearance of the anodic peak

The polarization curves obtained in this study made it evident the role played by each alloying in the alloy 22, when it is tested in media containing bicarbonate. From these tests was demonstrated that the anodic peak, which presents polarization curves of alloy 22, is due to the content of chromium not of molybdenum. As an example, Figure 12 shows polarization curves of the 22, Ni-Cr and Ni-Mo alloys in 1.148 mol/L NaHCO3 at 90°C. The figure shows the appearance of the anodic peak in the alloys containing chromium in its composition, while in the case of alloys containing only nickel and molybdenum the peak no appear. Ni-Cr alloys and alloy 22 showed similar curves, differing between them in the post-anode peak zone wherein the 22 alloy has current values above those of the Ni-Cr alloy. With the help of Pourbaix diagrams could relate the anodic peak with change in oxidation of Cr.

Figure 13 (Rincón Ortiz, 2011) shows the Pourbaix diagram of Cr modified to a temperature of 90 °C for analysis due to the intensity of peaks present in anodic curves performed at this temperature. When taking into account that the pH solution of tests is between 8 and 9.5, and that the potential range where the peak occurs is between +100 and +400 mV_{ECS}, it could relate anodic peak with chromium oxidation rate, which changes from Cr^{+3} (Cr_2O_3) to Cr^{+6} (CrO_4^{--}).

4.2. Temperature effect on the appearance of the anodic peak

All alloys, in all studied media presented a modification of the polarization curves when test temperature is modified. As the temperature decreased, the anodic peak of the alloys 22 and Ni-Cr shifted to higher potentials. The decreasing in temperature influence on the appearance of the anodic peak, making it less noticeable as the temperature decreases. The potential presented at the anodic peak showed an increase as the test temperature was reduced. This behavior was observed in both alloys for all media studied. As for the current density at which the peak occurs also changed with the modification in temperature of alloy 22. The current density in anodic peak of Ni-Cr alloy is approximately constant with temperature, in all media tested.

4.3. Effect of the concentration of the solutions in the appearance of anodic peak

As added chloride ions in the bicarbonate solution, the polarization curves of all alloys tested had modifications. As an example, in Figures 14 to 16, the variation of the polarization curves of alloys 22, Ni-Cr and Ni-Mo is presented, including concentration of the media, at 90 ° C. The Ni-Mo alloy showed a significant difference when the chloride concentration was 1 mol /L. At this concentration, polarization curve showed higher values of current density along the whole curve and was the condition that caused more superficially damage of sample tested, regardless of the test temperature. In the case of alloy 22, both the potential at which the peak occurs as the current density, increased with the concentration of chloride ions. This increase was more evident when the temperature was higher. A temperature of 90 °C, Ni-Cr alloy showed an increase in the potential and the current density of peak with the concentration of solution. At the temperatures of 75 °C, 60 °C and 25 °C, the current density increased with the addition of chloride in the media, while the anodic peak potential showed no clear trend with concentration of solutions.

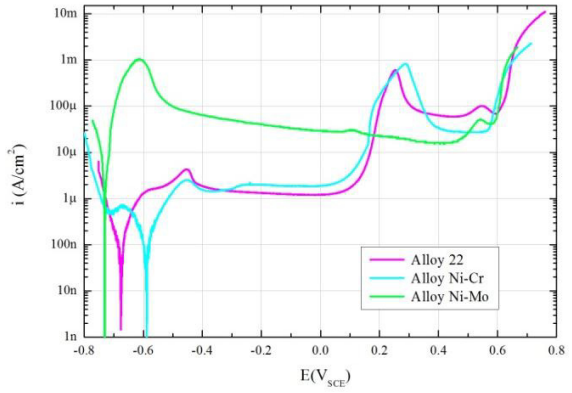

Fig. 12. Polarization curves of alloys 22, Ni-Cr and Ni-Mo in 1.148 mol/L $NaHCO_3$ at 90ºC.

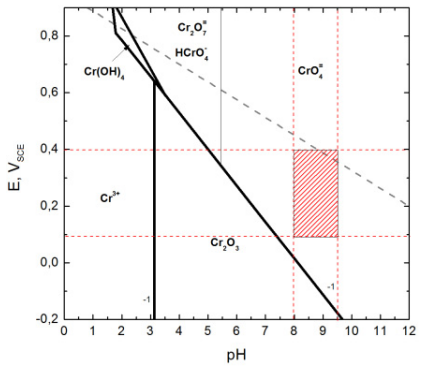

Fig. 13. Pourbaix diagram of Cr modified for temperature of 90°C. (Rincón Ortiz, 2011)

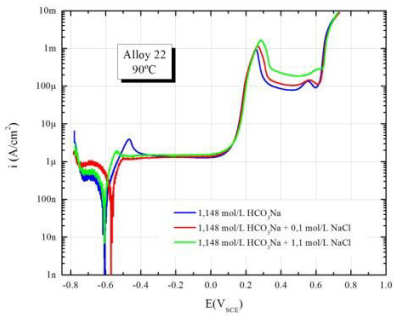

Fig. 14. Polarization curves of Alloy 22 in different media tested at 90°C

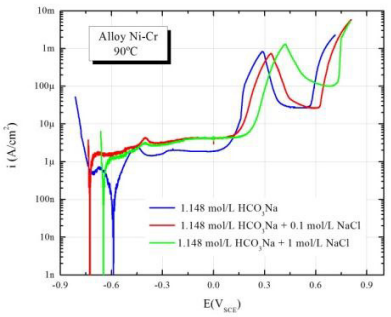

Fig. 15. Polarization curves of Ni-Cr alloy in different media tested at 90°C

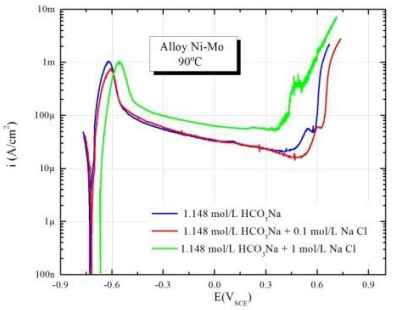

Fig. 16. Polarization curves of Ni-Mo alloy in different media tested at 90°C

5. Conclusions

- Was corroborated the correspondence between the bicarbonate ions and the presence of an anodic peak in the Alloy 22, in the region previous to transpassive zone. None of the studied alloys showed a peak when tested in medium containing chlorides.
- The anodic peak that has 22 alloy, when was tested in media containing bicarbonate was related to their content of Cr but was not related to Mo content. The Ni-Mo alloy did not show under any conditions tested, anodic peak similar to that presented 22 and Ni-Cr alloys.
- The anodic peak with change in chromium oxidation could be related with changes in Cr^{+3} (Cr_2O_3) to Cr^{+6} (CrO_4^{--}).
- The potential at which the anodic peak appeared in the 22 and Ni-Cr alloys varied with temperature and concentration of chloride ions in the medium. The peak potential always increased when the test temperature decreased. Alloy 22 showed an increased peak potential with the concentration of chloride ions. However, alloy 22 showed no relationship with concentration of the media.
- The current density at which the anodic peak appeared in the Ni-Cr alloy remained roughly constant with temperature, whereas alloy 22 was changed with temperature. The current density of peak increased with the concentration of solution in 22 and Ni-Cr alloys, at 90 °C.

References

ASTM G5-94, 2004, Standard Reference Test Method for Making Potentiostatic and Potentiodynamic Anodic Polarization Measurements" in Annual Book of ASTM Standards, vol. 03.02 (West Conshohocken, PA: ASTM Intl.), 53-64

Bodvarsson G., et al. 2003, Yucca Mountain Project, Elsevier.

Chiang K.T., Dunn D.S., Cragnolino G.A., 2005, Effect of groundwater chemistry on stress corrosion cracking, NACE Corrosion 2005, Paper 05463.

Chiang K.T., Dunn D.S., Cragnolino G.A., 2006, The combined effect of bicarbonate and chloride ions on the stress corrosion cracking susceptibility of alloy 22, NACE Corrosion 2006, Paper 06506. 1–20.

Chiang K.T., Dunn D.S., Cragnolino G.A., 2007, Effect of Simulated Groundwater Chemistry on Stress Corrosion Cracking of Alloy 22, Corrosion 63. 940–950.

Cragnolino G.A., Dunn D.S., Pan Y., 2003 Effects of Potential and Environment on Stress Corrosion Cracking Susceptibility of Nickel-Chromium-Molybdenum Alloys, NACE Corrosion 2003, Paper 03541.

Dunn D.S., Yang L., Pan Y., Cragnolino G.A., 2003 Localized Corrosion Susceptibility of Alloy 22, NACE Corrosion 2003, Paper 03697.

Dunn D.S., Pan Y., Chiang K.T., Yang L., Cragnolino G.A., He X., 2005. The localized corrosion resistance and mechanical properties of alloy 22 waste package outer containers, JOM Journal of the Minerals, Metals and Materials. 49 – 55.

Dunn D.S., Chiang K.T., Cragnolino G.A., 2006, Surface analysis of alloy 22 under conditions that promote stress corrosion cracking, NACE Corrosion 2006, Paper 06509. 1–11.

Estill J.C., King K.J., Fix D.V., Spurlock D.G., Hust G.A., Gordon S.R., 2002, Susceptibility of alloy 22 to environmentally assisted cracking in yucca mountain relevant environments, NACE Corrosion 2002, Paper 02535. 1–13.

Fix D.V., Estill J.C., Hust G.A., King K.J., Day S.D., Rebak R.B., 2003. Influence of Enviromental variables on the susceptibility of Alloy 22 to Environmentally Assisted Cracking, NACE Corrosion 2003, Paper 03688.

Fix D.V., Estill J.C., Hust G.A., Wong L.L., Rebak R.B., 2004, Environmentally assisted cracking behavior of nickel alloys in simulated acidic and alkaline ground waters using u-bend specimens, NACE Corrosion 2004, Paper 04549. 1–18.

Gordon G.M., 2002, Speller Award Lecture: Corrosion Considerations Related to Permanent Disposal of High-Level Radioactive Waste, Corrosion. 58 811–825.

King K.J., Wong L.L., Estill J.C., Rebak R.B.,2004, Slow Strain Rate Testing of Alloy 22 in Simulated Concentrated Ground Waters, NACE Corrosion 2004, Paper 04548. 1–16.

Rebak, R.B. 2003, Metallurgical effects on the behavior of nickel alloys, in: ASM Metals Handbook, Vol 13A, 279–286.

Rebak, R.B., 2005 Factors affecting the crevice corrosion susceptibility of alloy 22, NACE Corrosion 2005, Paper 05610. 1–17.

Rincón Ortiz M., 2011, Corrosión de una superaleación de Níquel en componentes de aguas subterráneas, in: Doctorado En Ciencia y Tecnología Mención Materiales, Instituto Sabato, UNSAM/CNEA

Rodríguez M.A., Carranza R.M., Rebak R.B., 2009, Crevice corrosion of Alloy 22 at the open circuit potenctial in hot chloride solutions, NACE Corrosion 2009, Paper 09424. 1–12.

Rodríguez M.A., Carranza R.M., Rebak R.B., 2010, Passivation and Depassivation of Alloy 22 in Acidic Chloride Solutions, Journal of The Electrochemical Society. 157, C1–C8.

Shukla P.K., Dunn D.S., Pensado O., 2006, Stress corrosion cracking model for alloy 22 in the potential yucca mountain repository environment, NACE Corrosion 2006, Paper 06502. 1–25.

Witherspoon P.A., Bodvarsson G.S., 2006, Geological Challenges in Radioactive Waste Isolation: Fourth Worldwide Review on, Earth Science Division. Ernest Orlando Lawrence Berkeley National Laboratory. University of California, Berkeley.

Zadorozne N. R. Rebak, M. Giordano, A. Ares and R. Carranza, 2012, Effect of temperature and chloride concentration on the anodic behavior of nickel alloys in bicarbonate solutions, Procedia Materials Science 1, 207 – 214.